

Nonideal strongly magnetized plasmas of neutron stars and their electromagnetic radiation

This article has been downloaded from IOPscience. Please scroll down to see the full text article.

2006 J. Phys. A: Math. Gen. 39 4453

(<http://iopscience.iop.org/0305-4470/39/17/S21>)

View [the table of contents for this issue](#), or go to the [journal homepage](#) for more

Download details:

IP Address: 171.66.16.104

The article was downloaded on 03/06/2010 at 04:24

Please note that [terms and conditions apply](#).

Nonideal strongly magnetized plasmas of neutron stars and their electromagnetic radiation

A Y Potekhin¹, G Chabrier², D Lai³, W C G Ho⁴ and M van Adelsberg³

¹ Ioffe Physico-Technical Institute, St Petersburg, Russia

² Ecole Normale Supérieure de Lyon, C.R.A.L.(UMR 5574 CNRS), France

³ Center for Radiophysics and Space Research, Department of Astronomy, Cornell University, Ithaca, NY 14853, USA

⁴ Hubble Fellow, MIT Kavli Institute for Astrophysics and Space Research, 77 Massachusetts Ave, 37-582F, Cambridge, MA 02139, USA

E-mail: palex@astro.ioffe.ru

Received 15 September 2005, in final form 8 November 2005

Published 7 April 2006

Online at stacks.iop.org/JPhysA/39/4453

Abstract

We study the equation of state, polarization and radiation properties for nonideal, strongly magnetized plasmas which compose outer envelopes of magnetic neutron stars. Detailed calculations are performed for partially ionized hydrogen atmospheres and for condensed hydrogen or iron surfaces of these stars.

PACS numbers: 52.25.Kn, 52.25.Xz, 52.25.Os, 97.10.Ex, 97.60.Jd

1. Introduction

Neutron stars can be considered as natural laboratories for studying the properties of matter under extreme physical conditions (see, e.g., [1]). In their cores the density ρ may exceed $10^{15} \text{ g cm}^{-3}$ and the temperature T lies typically between 10^7 and 10^9 K, but their thermal emission depends on the properties of the outer envelopes with lower ρ and T . The temperature decreases in the heat-blanketing envelopes (at $\rho \lesssim 10^8 \text{ g cm}^{-3}$) to $T \sim T_{\text{eff}}$ near the radiative surface (at $\rho \sim 10^{-3} - 10^6 \text{ g cm}^{-3}$, depending on the stellar parameters), where T_{eff} is the *effective surface temperature* related to the thermal flux through Stefan's law. In these envelopes, the magnetic field strength B may reach 10^{15} G; most often $B \sim 10^{11} - 10^{13}$ G. To calculate spectra of neutron-star emission that can be compared with the observations, one should take into account nonideality of the plasma in the envelopes and the effects of strong magnetic fields on the properties of the plasma and electromagnetic radiation.

In the cases where $T_{\text{eff}} \sim \text{a few} \times 10^5 - 10^6$ K (characteristic of middle-aged neutron stars, i.e., of age $\sim 10^4 - 10^6$ year) and $B \lesssim 10^{13}$ G, the spectrum of thermal emission from a neutron star forms in an stellar *atmosphere*. In a strong magnetic field, the state of matter can change

significantly (for review, see, e.g., [2]). For instance, at $T_{\text{eff}} \sim 10^6$ K, an atmosphere composed of hydrogen might be treated as fully ionized if the magnetic field were zero, but there can be a significant fraction of bound H atoms, if $B \gtrsim 10^{11}$ G. At lower T (characteristic of older stars) and sufficiently high B , *magnetic condensation* may occur, resulting in formation of a solid or liquid metallic surface, composed of a strongly coupled Coulomb plasma and covered by a thin gaseous atmosphere.

Although the possible importance of these effects was realized long ago, they were not included in neutron-star atmosphere models until recently (e.g. [3] and references therein). Early considerations of partial ionization in the magnetized neutron-star atmospheres (e.g. [4, 5]; also reviewed briefly in [6]) were not very reliable because of oversimplified treatments of atomic physics and nonideal plasma effects in strong magnetic fields. However, in the last decade the studies of dense nonideal plasmas in the strong magnetic fields made a spectacular progress which now allows one to calculate the spectrum and polarization of electromagnetic radiation formed in an extended partially ionized hydrogen atmosphere or emitted from a condensed metallic surface of a magnetic neutron star. In this paper, we briefly review these achievements.

2. Equation of state and opacities of partially ionized atmospheres with strong magnetic fields

Motion of electrons and ions in a magnetic field is quantized in the Landau orbitals. In neutron-star atmospheres, the field is usually *strongly quantizing* for the electrons (see, e.g., companion paper [7] for basic definitions). When $B \gg 10^9$ G, the properties of atoms and molecules change drastically [2]. In particular, the centre-of-mass motion of an atom is coupled to the internal degrees of freedom. This effect is important for both the equation of state (EOS) and radiative opacities of the plasma. In this section, we briefly review these effects for the case of the hydrogen plasma, the only one that has been studied in detail up to now. This case is quite realistic because even a small amount of hydrogen on the surface of the neutron star is sufficient to fill the entire atmosphere. For instance, for a ‘canonical’ neutron star (with mass $M = 1.4$ solar masses and radius $R = 10$ km), the total mass of the hydrogen atmosphere is $\sim 10^{12} \rho T_6$ g, where ρ is the bottom atmosphere density in g cm^{-3} and $T_6 = T_{\text{eff}}/10^6$ K. This mass of hydrogen can be accreted from the interstellar medium or from a nebula surrounding the star, or produced in spallation of heavy nuclei by highly energetic plasma discharges in the polar-cap regions of a pulsar.

2.1. Ionization equilibrium and equation of state

The EOS for partially ionized hydrogen at $10^{11} \text{ G} \lesssim B \lesssim 10^{13} \text{ G}$ was calculated and discussed in [8]; recently it was extended to the case $10^{13} \text{ G} \lesssim B \lesssim 10^{15} \text{ G}$ [9] and tabulated [9, 10]. The treatment is based on the free energy minimization. The free energy model is in essence a generalization of the nonmagnetic model of Saumon and Chabrier [12, 13]. We consider a plasma composed of N_p protons, N_e electrons, N_H hydrogen atoms and N_{mol} molecules in a volume V , the number densities being $n_j \equiv N_j/V$. The Helmholtz free energy is written as

$$F = F_{\text{id}}^{\text{e}} + F_{\text{id}}^{\text{p}} + F_{\text{id}}^{\text{neu}} + F_{\text{ex}}^{\text{C}} + F_{\text{ex}}^{\text{neu}}, \quad (1)$$

where F_{id}^{e} , F_{id}^{p} and $F_{\text{id}}^{\text{neu}}$ are the free energies of ideal gases of the electrons, protons and neutral species, respectively, F_{ex}^{C} takes into account the Coulomb plasma nonideality and $F_{\text{ex}}^{\text{neu}}$ is the nonideal contribution which arises from interactions of bound species with one another and with the electrons and protons. Ionization equilibrium is given by minimization of F

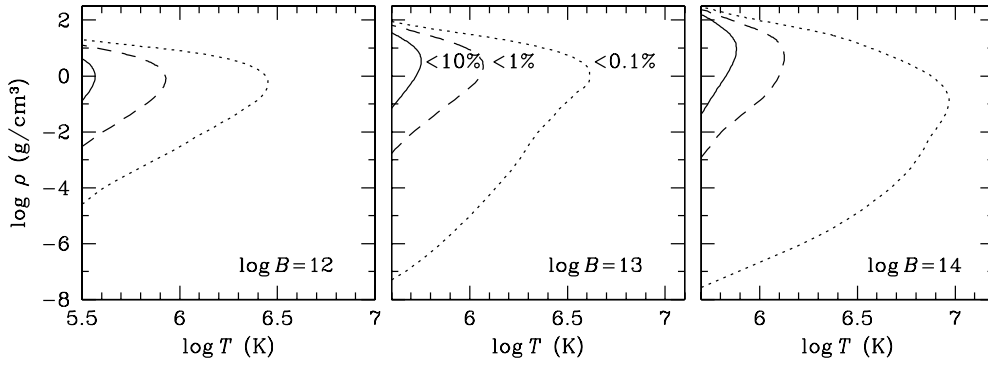


Figure 1. Domains of partial ionization in the ρ – T plane for $B = 10^{12}, 10^{13}$ and 10^{14} G. The contours delimit the domains where the atomic fraction $x_{\text{H}} < 0.1\%$ (to the right of the dotted lines), $0.1\% < x_{\text{H}} < 1\%$ (between the dashed and dotted lines), $1\% < x_{\text{H}} < 10\%$ (between the solid and dashed lines) or $x_{\text{H}} > 10\%$ (to the left of the solid lines).

with respect to particle numbers under the stoichiometric constraints, keeping V and the total number of protons (free and bound) constant. The formulae for each term in (1) are given in [8, 10]. The employed minimization technique is similar to that presented in [11] for the nonmagnetic case.

Once the free energy is obtained, its derivatives over ρ and T and their combinations provide the other thermodynamic functions. These functions are affected by the strong magnetic field. In the domain of strongly quantizing field ($\rho < \rho_B$, see [7]), the electron degeneracy is reduced and the EOS becomes softer than it would be at $B = 0$. If the field is weakly quantizing ($\rho \gtrsim \rho_B$), the second-order thermodynamic functions oscillate with increasing ρ around their field-free values (for details, see [8, 10]).

Figure 1 shows the domains of partial ionization in the ρ – T plane for different values of B . The higher the B , the greater the T at which the bound species are important. The calculated atomic fractions x_{H} are needed to obtain the radiative opacities in the atmosphere (see section 2.2).

Our model becomes less reliable at relatively low T where molecular chains H_n can be important [2]. Generally, this occurs within the ρ – T domain where $x_{\text{H}} \gtrsim 0.1$ (i.e. to the left of the solid lines in figure 1).

2.2. Radiative opacities, polarization and spectra

A magnetic field affects the properties of electromagnetic radiation in plasmas (e.g. [14]). At photon energies $\hbar\omega$ much higher than $\hbar\omega_{\text{pl}} = (4\pi\hbar^2 e^2 n_e / m_e)^{1/2} \approx 28.7\rho^{1/2}$ eV, where ω_{pl} is the electron plasma frequency and ρ is the density in g cm^{-3} , radiation propagates in the form of two so-called *normal modes*. These modes have different polarization vectors e_j and different absorption and scattering coefficients, which depend on the angle θ_B between the radiation propagation direction and the magnetic field. The two modes interact with each other via scattering.

In a partially ionized atmosphere, the opacity for each normal mode is contributed by electrons, ions and bound species. The scattering cross section includes contributions from the electrons and protons: $\sigma_{\alpha}^{\text{s}} = \sigma_{\alpha}^{\text{s,e}} + \sigma_{\alpha}^{\text{s,p}}$ (the subscript $\alpha = 0, \pm 1$ denotes a basic photon polarization—longitudinal, right or left circular—with respect to the magnetic field direction). The absorption cross section $\sigma_{\alpha}^{\text{a}}$ includes contributions from absorption

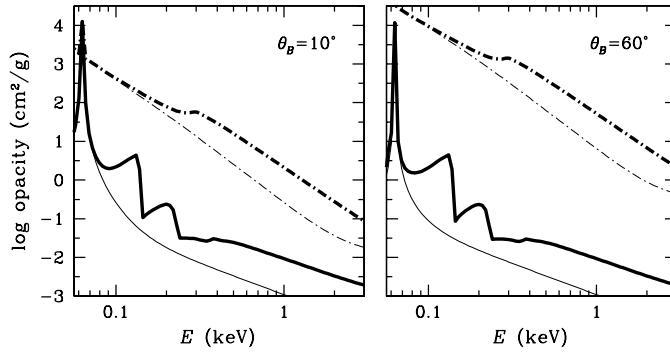


Figure 2. Radiative opacities of the plasma versus photon energy at $B = 10^{13}$ G, $\rho = 1 \text{ g cm}^{-3}$ and $T = 10^6$ K, for two values of the angle θ_B between the propagation direction and the magnetic field (left: $\theta_B = 10^\circ$; right: $\theta_B = 60^\circ$), for the ordinary (chain lines) and extraordinary (solid lines) normal mode of radiation. The case of partially ionized hydrogen plasma (thick lines) is compared with the approximation of fully ionized plasma (thin lines).

by plasma electrons and protons (mainly by free–free transitions due to the electron–proton collisions, $\sigma_\alpha^{\text{ff}}$), transitions between discrete states of an atom (bound–bound absorption, $\sigma_\alpha^{\text{bb}}$) and photoionization (bound–free, $\sigma_\alpha^{\text{bf}}$). Thus, for the hydrogen atmosphere, we can write $\sigma_\alpha^{\text{a}} \approx x_{\text{H}}(\sigma_\alpha^{\text{bb}} + \sigma_\alpha^{\text{bf}}) + (1 - x_{\text{H}})\sigma_\alpha^{\text{ff}}$. For the hydrogen in a strong magnetic field, the cross sections $\sigma_\alpha^{\text{bb}}$ were studied in [15], $\sigma_\alpha^{\text{bf}}$ in [16] and $\sigma_\alpha^{\text{ff}}$ in [10].

The bound species affect the dielectric tensor of the medium and hence the polarization properties of the normal modes. These effects were studied in [17], with use of the Kramers–Kronig relation between the imaginary and real parts of the plasma polarizability. The full account of the coupling of the quantum mechanical structure of the atoms to their centre-of-mass motion across the magnetic field proved to be crucial for the correct evaluation of the plasma polarization properties and opacities.

An example of the opacities is shown in figure 2. In this case, the ionization degree is high ($x_{\text{H}} = 0.016$), but the account of the bound species is still important: in the photon energy ranges corresponding to the bound–bound and bound–free atomic transitions, the model of a fully ionized plasma underestimates the opacities by a factor of ~ 10 .

These results are used in modelling the spectra of radiation from the neutron-star atmospheres [17, 18]. An example shown on the left panel of figure 3 clearly demonstrates the importance of the partial-ionization effects.

3. Radiation from the condensed surface in a strong magnetic field

The notion that an isolated magnetic neutron star has a condensed surface was first put forward by Ruderman [19], who considered the Fe surface. Lai and Salpeter [20] (see also [2]) studied the phase diagram of strongly magnetized hydrogen and showed that, if T_{eff} is below a critical value (which is a function of B), the atmosphere can undergo a phase transition into a condensed state. The thermal emission from the magnetized Fe surface was studied in [21–23] and most thoroughly in paper [24]. For a smooth condensed surface, the overall emission is reduced from the blackbody by less than a factor of 2, whereas for a rough surface, the reduction can be negligible (see [24]). The spectrum exhibits modest deviation from blackbody across a wide energy range, and shows mild absorption features associated with the ion cyclotron frequency

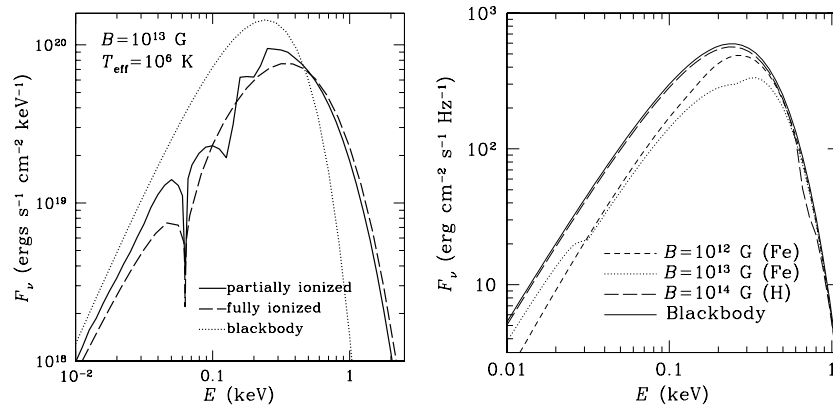


Figure 3. Spectral flux as a function of photon energy E . Left: the case of a partially ionized hydrogen atmosphere (solid line) at $B = 10^{13}$ G (field normal to the surface) and $T_{\text{eff}} = 10^6$ K is compared with the approximation of fully ionized plasma (dashes) and with the blackbody spectrum (dots). Right: the cases of condensed Fe ($B = 10^{12}$ G, short dashes; 10^{13} G, dots) and H ($B = 10^{14}$ G, long dashes) surfaces, at temperature $T = 10^6$ K, compared with the blackbody spectrum (solid line).

and the electron plasma frequency in the condensed matter. Examples of the spectrum for different models of the surface are shown on the right panel of figure 3.

4. Concluding remarks

We have briefly reviewed the main effects of strong magnetic fields on the EOS, opacities and properties of electromagnetic radiation in the surface layers of neutron stars. In order to calculate realistic spectra of thermal radiation from neutron stars, one must carefully take these effects into account. We expect that comparison of the calculated models with observations will help us to improve the constraints on neutron-star parameters (for example, their effective temperatures, see [7]) and thus provide a powerful tool for testing the theories of superdense matter in neutron-star interiors.

Acknowledgments

The work of GC was partially supported by the CNRS French–Russian grant PICS 3202. The work of AYP was partially supported by the RLSS grant 1115.2003.2 and the RFBR grants 05-02-16245, 03-07-90200 and 05-02-22003. WCGH is supported by NASA through Hubble Fellowship grant HF-01161.01-A awarded by the STScI, which is operated by the AURA, Inc., for NASA, under contract NAS 5-26555.

References

- [1] Shapiro S L and Teukolsky S A 1983 *Black Holes, White Dwarfs, and Neutron Stars: The Physics of Compact Objects* (New York: Wiley)
- [2] Lai D 2001 *Rev. Mod. Phys.* **73** 629
- [3] Pavlov G G, Shibano Yu A, Zavlin V E and Meyer R D 1995 *The Lives of the Neutron Stars* ed M A Alpar, Ü Kiziloğlu and J van Paradijs (Dordrecht:Kluwer) p 71
- [4] Miller M C 1992 *Mon. Not. R. Astron. Soc.* **255** 129

- [5] Rajagopal M, Romani R and Miller M C 1997 *Astrophys. J.* **479** 347
- [6] Zavlin V E and Pavlov G G 2002 *Proc. 270: WE-Heraeus Seminar on Neutron Stars, Pulsars, and Supernova Remnants (MPE Report vol 278)* ed W Becker, H Lesch and J Trümper (Garching: MPE) p 263
- [7] Chabrier G, Saumon D and Potekhin A Y this volume
- [8] Potekhin A Y, Chabrier G and Shibano Yu A 1999 *Phys. Rev. E* **60** 2193
- [9] Potekhin A Y and Chabrier G 2004 *Astrophys. J.* **600** 317
- [10] Potekhin A Y and Chabrier G 2003 *Astrophys. J.* **585** 955
- [11] Potekhin A Y 1996 *Phys. Plasmas* **3** 4156
- [12] Saumon D and Chabrier G 1991 *Phys. Rev. A* **44** 5122
- [13] Saumon D and Chabrier G 1992 *Phys. Rev. A* **46** 2084
- [14] Ginzburg V L 1970 *The Propagation of Electromagnetic Waves in Plasmas* (London: Pergamon)
- [15] Pavlov G G and Potekhin A Y 1995 *Astrophys. J.* **450** 883
- [16] Potekhin A Y and Pavlov G G 1997 *Astrophys. J.* **483** 414
- [17] Potekhin A Y, Lai D, Chabrier G and Ho W C G 2004 *Astrophys. J.* **612** 1034
- [18] Ho W C G, Lai D, Potekhin A Y and Chabrier G 2003 *Astrophys. J.* **599** 1293
- [19] Ruderman M 1971 *Phys. Rev. Lett.* **27** 1306
- [20] Lai D and Salpeter E E 1997 *Astrophys. J.* **491** 270
- [21] Brinkmann W 1980 *Astron. Astrophys.* **82** 352
- [22] Turolla R, Zane S and Drake J J 2004 *Astrophys. J.* **603** 265
- [23] Perez-Azorin J F, Miralles J A and Pons J A 2005 *Astron. Astrophys.* **433** 275
- [24] van Adelsberg M, Lai D, Potekhin A Y and Arras P 2005 *Astrophys. J.* **628** 902